DOI 10.1002/pmic.201200041 *Proteomics* 2012, *12*, 1928–1937

RESEARCH ARTICLE

Comparative label-free LC-MS/MS analysis of colorectal adenocarcinoma and metastatic cells treated with 5-fluorouracil

Kerry M. Bauer, Paul A. Lambert and Amanda B. Hummon

Department of Chemistry and Biochemistry, University of Notre Dame, Notre Dame, IN, USA

A label-free mass spectrometric strategy was used to examine the effect of 5-fluorouracil (5-FU) on the primary and metastatic colon carcinoma cell lines, SW480 and SW620, with and without treatment. 5-FU is the most common chemotherapeutic treatment for colon cancer. Pooled biological replicates were analyzed by nanoLC-MS/MS and protein quantification was determined via spectral counting. Phenotypic and proteomic changes were evident and often similar in both cell lines. The SW620 cells were more resistant to 5-FU treatment, with an IC_{50} 2.7-fold higher than that for SW480. In addition, both cell lines showed pronounced abundance changes in pathways relating to antioxidative stress response and cell adhesion remodeling due to 5-FU treatment. For example, the detoxification enzyme NQO1 was increased with treatment in both cell lines, while disparate members of the peroxiredoxin family, PRDX2 or PRDX5 and PRDX6, were elevated with 5-FU exposure in either SW480 or SW620, respectively. Cell adhesion-associated proteins CTNNB1 and RhoA showed decreased expression with 5-FU treatment in both cell lines. The differential quantitative response in the proteomes of these patient-matched cell lines to drug treatment underscores the subtle molecular differences separating primary and metastatic cancer cells.

Received: January 31, 2012
Revised: February 27, 2012
Accepted: March 5, 2012

Keywords:
Bioanalytical methods / Cell biology / Colon cancer / 5-Fluorouracil / Label-free quantification / Mass spectrometry

1 Introduction

In 1971, the National Cancer Act was signed, signaling the beginning of a concentrated effort to study and understand cancer. Forty years later, progress has been made in understanding the complexities of cancer progression, but much remains to be learned regarding the molecular basis of these destructive malignancies. One of the deadliest cancers is colorectal cancer (CRC), which is the second leading cause of cancer-related deaths in the United States [1]. In 2011 alone, there were an estimated 100 000 new cases diagnosed and 49 000 deaths [1]. Progress in diagnosis and treatment has enabled clinicians to extend and save the lives of many patients at the early stages of this disease; however, the prognosis for patients with advanced disease or systemic metastasis is still very poor.

The most common therapeutic agent used to treat CRC is 5-fluorouracil (5-FU). 5-FU has been used for more than 40 years. 5-FU affects metabolic pathways and displays cytotoxic modes of action through the inhibition of thymidylate synthase activity and incorporation into RNA and DNA. 5-FU also induces cancer cells to undergo apoptosis in response to RNA and DNA damage [2]. Patient responses to 5-FU vary widely in terms of both efficacy and toxicity; response rates for 5-FU-based chemotherapy are only 10–15% [3]. Tumors may develop resistance to 5-FU over the course of treatment. Drug resistance, as well as metastatic spread of tumors to secondary sites, accounts for much of the morbidity and mortality associated with CRC.

Correspondence: Dr. Amanda B. Hummon, Department of Chemistry and Biochemistry, University of Notre Dame, 251 Nieuwland Science Hall, Notre Dame, IN 46556, USA
E-mail: ahummon@nd.edu
Fax: 574-631-6652

Abbreviations: CRC, colorectal cancer; **5-FU**, 5-fluorouracil; **GO**, gene ontology

The response of CRC cells to 5-FU has previously been examined; recently, a large panel of 77 CRC cell lines were treated with 5-FU and then tested for toxicity [4]. Another study compared the response of primary versus metastatic CRC lesions. Using a cohort of nonpatient-matched biopsies, the resected tumors were cultured in vitro, treated with 5-FU, and then tested for growth inhibition. Cells from metastatic lesions were found to be more resistant to 5-FU than those from primary tumors; however, the authors note that patient-matched comparisons of primary and metastatic lesions would be more informative than comparing lesions across different patients [5].

A useful patient-matched model for studying CRC metastasis is the cell lines, SW480 and SW620, isolated from the primary colon adenocarcinoma and the lymph node metastasis, respectively [6]. The primary SW480 cell line was derived from a Dukes' type B colon adenocarcinoma and the metastatic SW620 cell line was established from the same patient 1 year later. Due to the isogenic nature of these two cell lines, variation from genetic background is avoided, making them excellent models to study 5-FU treatment effects on primary and metastatic colon cancer. In addition, since chemotherapy was not started with the patient until after both biopsies were collected, no drug-induced alterations in gene expression are present.

While examining the effect of 5-FU on cell growth is valuable, understanding the molecular and especially the proteomic basis for metastasis and drug resistance may lead to improvement in the treatment of CRC. Previous studies have examined the basal proteomic differences between the SW480 and SW620 cell lines [7–9]. In addition, the proteomic changes that occur with 5-FU treatment in SW480 have been characterized [10].

These studies have largely relied on protein separations and comparison based on 2D PAGE followed by MS-based identification of specific excised protein spots. Alternatively, the field of MS-based quantification has grown significantly in recent years [11]. Quantitative proteomics via MS can be accomplished through three main methods: the use of a chemical [12] or metabolic [13] labeling strategy or a label-free technique. Label-free proteomic profiling offers several advantages over labeling techniques such as less complex sample preparation and lower reagent costs. The approach also does not suffer from the possibility of incomplete labeling. Label-free quantification can further be divided into two major groups: signal intensity measurement based on mass spectra and spectral counting. Spectral counting relative protein quantification is based on counting the number of identified MS/MS spectra assigned to a protein in an MS/MS experiment. This quantification technique is supported by the observation that more abundant peptides will be more readily selected for fragmentation. These peptides will produce a higher abundance of MS/MS spectra that are therefore directly proportional to protein amount in data-dependent acquisition. Relative protein abundance and spectral count is shown to have a strong, positive linear correlation with an r^2 value of 0.9997, and a dynamic range over two orders of magnitude [14]. Moreover, spectral counting has proved to be more reproducible and has a higher dynamic range compared to peptide ion chromatogram-based quantification [15]. Several excellent reviews have recently been written on the use of label-free mass spectrometric approaches and their applications in biological research [16–18].

As previously mentioned, 5-FU is the primary treatment option for patients with CRC, yet there are substantial variations in response to the drug, including among primary and metastatic lesions [5]. We sought to determine whether there exist proteomic differences between primary and metastatic CRC underlying this differential phenotypic response. To investigate this question, we used SW480 and SW620 and examined their proteomic profiles before and after 5-FU treatment using label-free, spectral counting-based quantitative MS.

2 Materials and methods

2.1 Cell culture

Colon cancer cell lines SW480 and SW620 were purchased from the American Type Culture Collection (ATCC, Manassas, VA, USA) and maintained in RPMI 1640 medium (Invitrogen, Gaithersburg, MD, USA) supplemented with 10% fetal bovine serum (Thermo Scientific, Pittsburgh, PA, USA) and 2 mM L-glutamine (Invitrogen) and grown in 5%CO_2 at 37°C. Cell lines were used within 3 months after receipt or resuscitation of frozen aliquots thawed from liquid nitrogen. The provider assured the authentication of these cell lines by cytogenetic analysis.

2.2 Dose–response curves of cells to 5-FU

SW480 or SW620 cells were seeded into 96-well plates at a concentration of 5000 cells/well and allowed to attach for 24 h. A range of concentrations (0.04, 0.08, 0.16, 0.31, 0.62, 1.3, 2.5, 5.0, 10.0, 20.0, 40.0, 80.0, 160.0, 320.0, 640.0, 1280.0, and 2560.0 μM) of 5-FU (Sigma-Aldrich, St. Louis, MO, USA) were prepared by dissolving in nanoPure water and added to RPMI 1640 medium. The 5-FU solutions were then added to the seeded cells and incubated for 72 h. As a surrogate marker for cell viability, the reduction of resazurin to resorufin was measured in cells using the Cell Titer-Blue Cell Viability assay (Promega, Madison, WI, USA). After 72 h of 5-FU treatment, reduction of resazurin to resorufin, read as fluorescence (560Ex/590Em), was measured using a plate reader (Spectramax M5; Molecular Devices, Sunnyvale, CA, USA). Viability of 5-FU-treated cells was compared to cells incubated without 5-FU. Triplicate measurements were collected for each concentration of 5-FU.

2.3 Treatment of cells with 5-FU

5-FU was dissolved in nanoPure water and added to RPMI 1640 medium at a final concentration of the determined IC_{50} for each cell line (SW480 IC_{50} was 7.5 μM; SW620 IC_{50} was 20.0 μM), whereas the same volume of RPMI 1640 medium without 5-FU was added to the control cells. The RPMI 1640 medium with and without 5-FU was added to the SW480 and SW620 test and control culture plates after incubating the seeded cells for 24 h. All culture plates were then incubated for 72 h. Triplicate biological replicates of both treated and untreated cells for each cell line were performed.

2.4 Cell lysis and protein sample preparation

After 72-h incubation, the culture medium was aspirated and the cells were rinsed with PBS (Invitrogen). Complete Lysis-M Reagent Kit (Roche Diagnostics, Indianapolis, IN, USA) with 1X Complete Protease Inhibitor (Roche Diagnostics) was added to each culture plate and incubated for 5 min at room temperature on a plate shaker. The cells were scraped, collected, and centrifuged at 15 000 rpm for 10 min to obtain soluble protein fractions. The total protein concentration of each sample was determined using a BCA protein assay kit (Thermo Scientific) and bovine serum albumin standard (Thermo Scientific) according to the manufacturer's instructions. Biological replicates for each sample were pooled with equal contribution from each biological replicate forming the pool. Twenty micrograms of each pooled protein sample were resolved by a NuPAGE SDS-PAGE system (Invitrogen) (4–12% acrylamide, Bis-Tris with MOPS running buffer) in two lanes each. After electrophoresis, the gel was stained with Colloidal Blue staining kit (Invitrogen) and washed with distilled water. The gel lanes corresponding to each sample were excised into five bands based on staining intensity. Each band was cut into 2 mm wide pieces and subjected to in-gel tryptic digestion. HPLC-grade water and ACN (Honeywell Burdick & Jackson, Muskegon, MI, USA) were used in the subsequent digestion. Gel pieces were washed/dehydrated three times in 50 mM ammonium bicarbonate (ABC) (Sigma-Aldrich)/50 mM ABC + 50% ACN. Cysteine bonds were reduced with 10 mM DTT (dithiothreitol) (Sigma-Aldrich) for 1 h at 56°C and alkylated with 55 mM IAA (iodoacetamide) (Sigma-Aldrich) for 20 min at room temperature in the dark. Following two subsequent wash/dehydrate cycles, the reduced and alkylated proteins were dried 20 min in a MiVac sample concentrator (Genevac Inc., New York, NY, USA) and incubated overnight with 12.5 ng/μL trypsin in 25 mM ABC at 37°C. Peptides were extracted twice in 50 μL of 50% ACN/45% water/5% formic acid (Optima LC/MS, Fischer Scientific, Fair Lawn, NJ, USA). The combined volumes were reduced to 15 μL in a speedvac. Peptides were desalted with C18 ZipTips (Millipore, Billerica, MA, USA) according to manufacturer's instructions. The desalted peptide volume was concentrated in a speedvac and the final volume was diluted to 10 μL with 0.1% formic acid.

2.5 Liquid chromatography/MS analysis of protein digests

Liquid chromatography was performed using a nanoAcquity ultra performance LC system (Waters, Milford, MA, USA) under the control of Hystar (Bruker Daltonics Ltd., MA, USA). Peptides were loaded onto a 75 μm C18 BEH nanoAcquity column (Waters) and trapped for 12 min at 500 nL/min at 95% buffer A (buffer A, 3% ACN and 0.1% formic acid; buffer B, 93% ACN and 0.1% formic acid) and separated at 500 nL/min in a 95–15% buffer A gradient in 55 min. Solvent A was held at 15% for 5 min to wash the column followed by 5 min at 95% buffer A to equilibrate the column before the next injection. The LC system was interfaced via the nanoESI spray source with a 3D high-capacity ion trap mass spectrometer (amaZon X, Bruker Daltonics). Mass spectra were acquired from 350 to 1800 m/z using parameters optimized at 922 m/z with a target of 200 000 set for ion charge control and a maximum acquisition time of 100 ms. The six most abundant precursor ions above a threshold of 50 000 were selected for MS/MS per MS scan with active exclusion for 45 s after selection. SmartFrag controlled the fragmentation of each precursor ion using helium gas and a 60–180% collision energy range with an amplitude of 1.0 V. Each sample was injected multiple times with data collected for each injection, providing three technical replicates per sample.

2.6 Data processing for protein identification and quantification

Raw LC-MS/MS data were processed automatically using DataAnalysis 4.0 software (Bruker Daltonics), with the following parameters: compounds (autoMSn) threshold 1000, number of compounds unlimited, retention time windows 1 min. Database searches were performed using an in-house Mascot v.2.3 search engine (Matrix Science, London, UK) and the human SwissProt database (v. 2.2.04), with the following parameters: tryptic peptides with up to two missed cleavage sites, peptide tolerance 1.3 Da, fragment tolerance 0.8 Da, $^{13}C = 1$, instrument type: ESI-TRAP, variable modifications: cysteine and N-terminal carbamidomethyl, methionine oxidation, asparagine, and glutamine deamination. All proteins were identified with a false discovery rate of <2% based on a decoy database search.

Bruker raw data files were converted to mzXML format using the msConvert tool of the ProteoWizard library. Label-free comparative and quantitative analysis was performed using the ProteoIQ software (v.2.3.01 BIOINQUIRE, Athens, GA, USA). A protein project was created in ProteoIQ after uploading the spectral data in mzXML format and the Mascot search results in .dat format. ProteoIQ was used to cluster

peptides to proteins (protein groups) and output lists of proteins having a minimum peptide probability of <0.05 and a minimum protein probability of <0.5. Spectral counting and related quantification data were generated and extracted for comparative analysis of SW480 and SW620 cell lines with and without 5-FU treatment. ProteoIQ kept track of spectral counts from each replicate, and then spectral counts were averaged between LC/MS runs. The average spectral count for each individual protein within a biological group was normalized by comparing the total spectral counts for all proteins identified in each biological group and replicate.

2.7 Validation by Western blot

Equal amounts of pooled soluble protein fractions from all four biological groups (SW480 and SW620 5-FU-treated and control harvested cells) were resolved on a 1-D SDS-PAGE gel. Upon completion of electrophoresis, the proteins were transferred to nitrocellulose membrane for 90 min at 12 V. The membrane was incubated with rabbit anti-β-catenin (1:5000) (Abcam, Cambridge, MA, USA), mouse anti-PRDX5 (1:1000) (GenWay Biotech, San Diego, CA, USA), rabbit anti-COX IV (1:1000) (Abcam), and rabbit anti-β-actin (1:1000) (Abcam) in 10% milk buffer in 1X PBS on a rocking platform overnight at 4°. The membrane was washed three times for 10 min in 10% milk buffer in 1X PBS and incubated with HRP-conjugated antimouse IgG (1:10 000) (Jackson ImmunoResearch West Grove, PA, USA) or HRP-conjugated antirabbit IgG (1:10 000) (Cell Signaling Technologies, MA, USA) for 1 h on a rocking platform at room temperature. The membrane was washed as before, rinsed with DI water and incubated with SuperSignal West Pico Chemiluminescent Substrate (Pierce/Thermo Fisher Scientific, Rockford, IL, USA) according the protocol. Kodak BioMax Light Film (Carestream Health Woodbridge, CT, USA) was used to expose the membrane for varying amounts of time. The film was developed using GBX developer and fixer (Carestream Health) according to their protocol.

3 Results and discussion

3.1 Determining the sensitivity of primary and metastatic colon cancer cells to 5-FU

Primary SW480 and metastatic-derived SW620 5-FU drug sensitivities were determined following in vitro treatment of the cells with 5-FU over a range of drug concentrations for 72 h. Cell viability was evaluated and the dose–response curves were plotted (Fig. 1). The IC_{50} values, the concentration of 5-FU that reduces cell viability by 50%, of the two cell lines were determined to be 7.5 μM for SW480 and 20.0 μM for SW620. The metastatic SW620 cell line is more resistant to 5-FUs cytotoxic effects as its IC_{50} is 2.7-fold higher than that of the primary SW480 cell line.

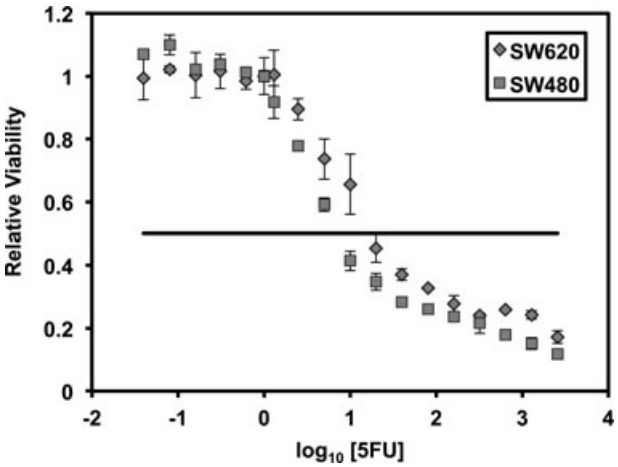

Figure 1. SW480 and SW620 human colon cell line dose–response curves to 5-FU treatment. The cell viability of 5-FU-treated cells is expressed as a percentage relative to control cells incubated without 5-FU. The 5-FU IC_{50} of SW480 and SW620 were determined to be 7.5 and 20.0 μM, respectively. Triplicate measurements were collected for each concentration of 5-FU. Error bars represent the median of three measurements. The horizontal line represents 50% viability.

3.2 Identification of differentially expressed proteins between 5-FU-treated and control SW480 and SW620 cells

To analyze the proteomic basis for the differential sensitivity, global protein analysis of the two cell lines with and without 5-FU treatment was conducted. For each cell line and treatment condition, pooled samples consisting of three biological replicates were used. Pooling the biological replicates reduces the biological variation within the sample and increases the power to detect changes in expression seen in the average sample above any noise from random biological variation. The use of three technical replicates allows identification of expression changes in the sample above the technical noise of the instrument [19]. Proteins with multiple annotated forms identified were clustered into protein groups to address the peptide centric nature of the samples. As the human proteome has much sequence redundancy, the same peptide sequence can be present in multiple different proteins or protein isoforms; these shared peptides lead to ambiguities in determining identities and abundance of proteins [20]. To increase protein identification capacity, dynamic exclusion is widely used. Dynamic exclusion will also result in a decrease of total spectral counts. However, it has been shown that protein expression ratios are not affected by dynamic exclusion [21]. Furthermore, enabling dynamic exclusion leads to higher peptide counts and a gain in quantification of lower abundance proteins [22].

In total, 900 protein groups were identified among the four biological conditions. Gene ontology (GO) analysis of

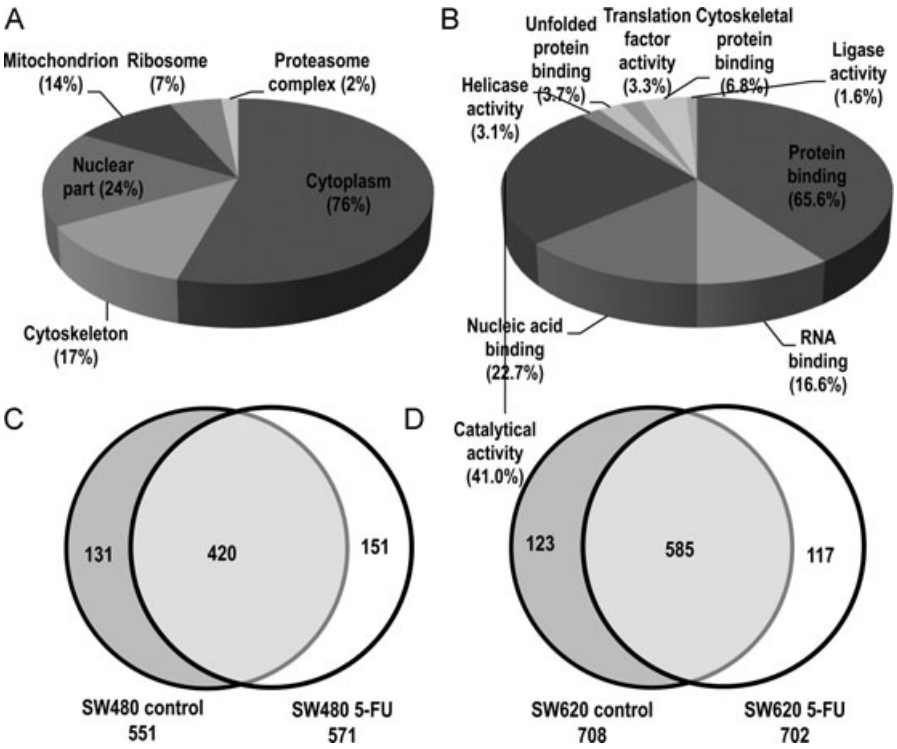

Figure 2. Gene ontology (GO) analysis and biological sample distribution of identified protein groups. The protein groups identified were classified by (A) broad subcellular localization and (B) molecular function. Some proteins may be represented in more than one category. The numbers in parentheses indicate the percentage of identified proteins represented by each category. Venn diagrams showing distribution of identified protein groups across the biological samples (C) SW480 and (D) SW620.

the protein groups identified the cellular compartments and biological processes represented by the proteins in the dataset (Fig. 2A and B). Specifically, identified protein groups assigned to cellular compartments were distributed among cytoplasmic (76%), nuclear (24%), cytoskeletal (17%), mitochondrial (14%), ribosomal (7%), and proteasome complex (2%) species, showing sufficient extraction and detection based on the wide distribution of identified protein groups. A large percentage of the identified proteins mapped to protein binding (65.5%), catalytic activity (41.0%), and nucleic acid binding (22.7%) species. The overlaps among the protein sets for the biological conditions are shown in Venn diagrams (Fig. 2C and 2D). There were a total of 702 protein groups identified in the SW480 sample set, 420 of which were identified in both 5-FU-treated and control samples. In the SW620 sample set, 825 protein groups were identified, with 585 identified in both 5-FU-treated and control samples. Protein group overlap evaluation between the technical triplicate runs is displayed in Supporting Information Fig. S1. Additional information regarding the protein groups identified can be found in Supporting Information Tables S1–S3. The respective protein group identifications are based on LC-MS/MS peptide fragmentation spectra. Representative fragment ion spectra of select peptide ions from several proteins show extensive fragmentation series of b- and y-ions (Supporting Information Fig. S2).

3.3 Spectral counting relative quantification

To quantify the identified proteins using spectral counting, the spectral counts of each peptide were averaged over its appearance in all technical replicates. To account for any deviation in technical reproducibility, the average spectral counts were normalized to the total number of spectral counts for each biological condition prior to relative protein quantification. The sum of the spectral counts from the constituent peptides of each protein was also calculated. A total of 900 protein groups were identified in this study; however, only a fraction of those proteins were accepted for quantification after applying a threshold of $\geq$4 SpC for high confidence in differential protein expression [23] (Supporting Information Fig. S3). A traditional twofold change in relative expression was set for identification of differentially expressed proteins. With these criteria, there were 267 protein groups accepted for quantification between the SW480-treated and -untreated samples and 401 protein groups accepted between the treated and untreated SW620 samples (Table 1). The distributions of expression changes for the protein groups are shown in Fig. 3. We found that only a small percentage of confidently quantifiable proteins were differentially expressed in the 5-FU-treated cells for both cell line comparisons. There were 51 protein groups whose expression changed with 5-FU treatment in the SW480 cell line comparison; 29 (10.9%) were upregulated and 27 (10.1%) were downregulated. In the SW620 cell line

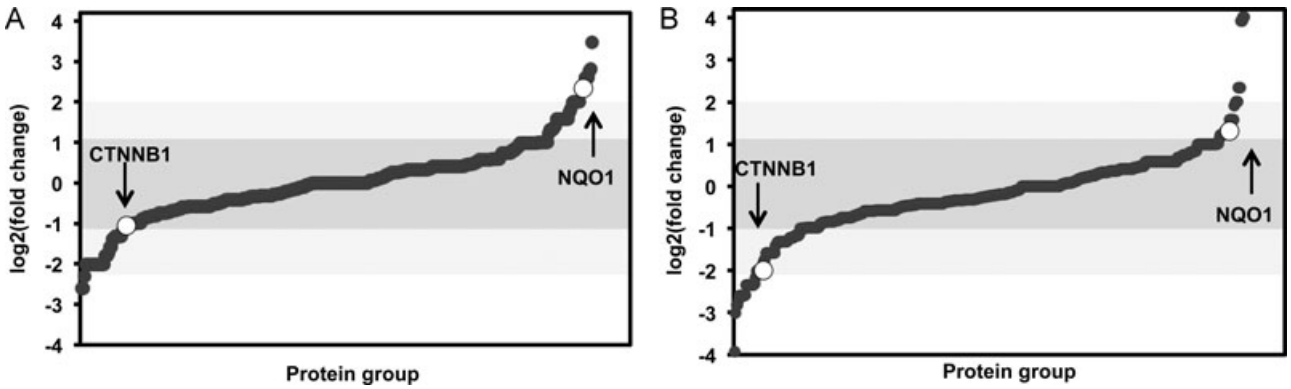

Figure 3. Distribution of protein group spectral count relative expression changes between (A) SW480 (B) and SW620 5-FU-treated as compared to control cells. The protein expression ratios are shown in $\log_2$ scale for all protein groups accepted for quantification. Protein ratios arranged from descending to ascending order results in a sigmoidal shaped curve. The darker shaded area represents unregulated protein groups with a less than twofold change in expression, with the lighter shaded area representing protein groups regulated between two- and threefold change. The expression ratios for NQO1 and CTNNB1 are indicated.

comparison, 79 protein groups showed changed expression; 22 (5.5%) were upregulated and 57 (14.2%) were downregulated. Highlighted are two proteins found to be upregulated (NQO1) or downregulated (CTNNB1) in both SW480 and SW620 5-FU-treated cells as compared to the control cells.

3.4 Functional annotation of protein groups with changed expression

GO annotation was used to analyze the function of differentially expressed protein groups. Pairwise analysis between control and 5-FU comparative protein expression profiling for each cell line revealed significant changes in proteins involved in cell adhesion remodeling (CTNNB1, RHOA) and antioxidant activity (NQO1,PARK7, PRDX2, PRDX5, PRDX6).

3.5 Cell adhesion remodeling

The chemosensitivity of cancer cells may be affected by the state of cell adhesion and expression of intracellular adhesion and cytoskeletal proteins. CTNNB1 (Catenin-beta 1) is a dual-purpose protein playing a critical role in the Wnt-signaling pathways and cell–cell adhesion. In epithelial cells, cytoplasm CTNNB1, a component of the adherens junctions, provides a mechanical linkage between cell-to-cell junction proteins and cytoskeletal proteins. Loss of CTNNB1 may result in cells that are less epithelial and more mesenchymal with disassembled cell-to-cell junctions and greater migratory properties. Epithelial to mesenchymal transition (EMT) has been shown to be correlated with anticancer drug resistance in several solid tumors including colon cancer [24]. The reduced expression of CTNNB1 in both SW480 and SW620 5-FU-treated cells, whether the result of increased activity of Wnt-regulated degradation or nuclear localization, may be compromising the epithelial integrity by interfering with the

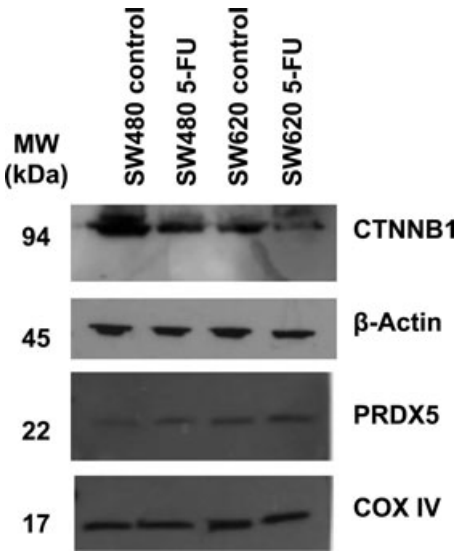

Figure 4. Western blot validation of selected proteins. Protein samples from SW480 and SW620 control and 5-FU-treated cell lysates were probed CTNNB1 and PRDX5 antibodies. β-Actin and COX IV were treated as loading controls.

cadherin–catenin interaction. Validation of the changes in CTNNB1 abundance with 5-FU treatment by Western blot is shown in Fig. 4.

RhoA is another cell adhesion protein showing decreased expression in the 5-FU-treated cells from both cell lines. This Rho GTPase is known to regulate the actin cytoskeleton through the formation of stress fibers and loss of RhoA results in the breakdown of adherens junctions [25]. The cells surviving 72 h of 5-FU treatment possibly represent cells with de novo resistance. Over time, the tumor acquires resistance and associated phenotypes such as EMT with major cell adhesion remodeling become more prominent. However, clues are present in the primary resistant cells as seen in the reduced expression of CTNNB1 and RhoA.

Table 1. Proteins identified with ≥4 SpC and a greater than twofold change in relative expression between 5-FU-treated and control samples for both SW620 (A) and SW480 (B) cells as determined by spectral counting

Accession	Gene name	Protein name	$\log_2$ ratio	*p*-Value
(A) SW620				
O75369	FLNB	Filamin-B	4.01	2.48×10^{-2}
P48444	COPD	Coatomer subunit delta	2.34	1.15×10^{-1}
Q04917	1433F	14-3-3 protein eta	2.34	7.41×10^{-2}
Q9Y262	EIF3L	Eukaryotic translation initiation factor 3 subunit L	2.34	2.37×10^{-2}
O00148	DDX39	ATP-dependent RNA helicase DDX39	2.01	5.06×10^{-2}
P30740	ILEU	Leukocyte elastase inhibitor	2.01	5.06×10^{-2}
P48681	NEST	Nestin	1.99	5.06×10^{-2}
Q14204	DYHC1	Cytoplasmic dynein 1 heavy chain 1	1.91	7.09×10^{-3}
Q6P2E9	EDC4	Enhancer of mRNA-decapping protein 4	1.58	1.37×10^{-1}
Q9Y230	RUVB2	RuvB-like 2	1.58	5.81×10^{-2}
Q99873	ANM1	Protein arginine N-methyltransferase 1	1.58	5.81×10^{-2}
P15559	NQO1	NAD(P)H dehydrogenase [quinone] 1	1.32	1.74×10^{-1}
O14818	PSA7	Proteasome subunit alpha type-7	1.32	1.74×10^{-1}
P02788	TRFL	Lactotransferrin	1.32	5.06×10^{-2}
P60660	MYL6	Myosin light polypeptide 6	1.32	5.06×10^{-2}
P46940	IQGA1	Ras GTPase-activating-like protein IQGAP1	1.25	6.46×10^{-4}
Q13813	SPTA2	Spectrin alpha chain, brain	1.22	1.87×10^{-1}
P00492	HPRT	Hypoxanthine-guanine phosphoribosyltransferase	1.22	5.81×10^{-2}
P32119	PRDX2	Peroxiredoxin-2	1.14	5.06×10^{-2}
P02771	FETA	Alpha-fetoprotein	1.01	1.47×10^{-1}
P33993	MCM7	DNA replication licensing factor MCM7	1.01	9.91×10^{-2}
Q9BSJ8-2	ESYT1	Isoform 2 of extended synaptotagmin-1	1	1.75×10^{-1}
Q99714	HCD2	3-Hydroxyacyl-CoA dehydrogenase type-2	−1.14	2.75×10^{-2}
P30050	RL12	60S ribosomal protein L12	−1.17	1.19×10^{-1}
O14980	XPO1	Exportin-1	−1.17	9.45×10^{-2}
P17844	DDX5	Probable ATP-dependent RNA helicase DDX5	−1.17	4.17×10^{-2}
P27824	CALX	Calnexin	−1.17	3.34×10^{-2}
P37837	TALDO	Transaldolase	−1.22	1.37×10^{-1}
P04843	RPN1	Dolichyl-diphosphooligosaccharide subunit 1	−1.22	1.37×10^{-1}
P41252	SYIC	Isoleucyl-tRNA synthetase, cytoplasmic	−1.22	1.03×10^{-1}
P26640	SYVC	Valyl-tRNA synthetase	−1.22	1.03×10^{-1}
P25205	MCM3	DNA replication licensing factor MCM3	−1.22	5.81×10^{-2}
Q15758	AAAT	Neutral amino acid transporter B(0)	−1.25	1.47×10^{-2}
P50990	TCPQ	T-complex protein 1 subunit theta	−1.28	8.61×10^{-3}
P63010-2	AP2B1	Isoform 2 of AP-2 complex subunit beta	−1.32	1.74×10^{-1}
P25789	PSA4	Proteasome subunit alpha type-4	−1.32	1.25×10^{-1}
P46783	RS10	40S ribosomal protein S10	−1.32	1.25×10^{-1}
P62851	RS25	40S ribosomal protein S25	−1.32	1.25×10^{-1}
P56192	SYMC	Methionyl-tRNA synthetase, cytoplasmic	−1.32	1.25×10^{-1}
P33992	MCM5	DNA replication licensing factor MCM5	−1.32	5.06×10^{-2}
P13797	PLST	Plastin-3	−1.32	5.06×10^{-2}
P63244	GBLP	Guanine nucleotide-binding protein subunit beta-2-like 1	−1.32	1.12×10^{-2}
P17987	TCPA	T-Complex protein 1 subunit alpha	−1.32	8.01×10^{-3}
P22234	PUR6	Multifunctional protein ADE2	−1.38	6.22×10^{-2}
P60228	EIF3E	Eukaryotic translation initiation factor 3 subunit E	−1.42	1.19×10^{-1}
P00367	DHE3	Glutamate dehydrogenase 1	−1.58	7.92×10^{-2}
Q13283	G3BP1	Ras GTPase-activating protein-binding protein 1	−1.58	5.81×10^{-2}
Q9Y617	SERC	Phosphoserine aminotransferase	−1.58	5.81×10^{-2}
P08195-4	4F2	Isoform 4 of 4F2 cell-surface antigen heavy chain	−1.58	1.81×10^{-2}
Q15366	PCBP2	Poly(rC)-binding protein 2	−1.58	1.29×10^{-2}
P51149	RAB7A	Ras-related protein Rab-7a	−1.59	1.95×10^{-2}
O00571	DDX3X	ATP-dependent RNA helicase DDX3X	−1.74	1.10×10^{-3}
Q16555	DPYL2	Dihydropyrimidinase-related protein 2	−1.76	5.06×10^{-2}
P26196	DDX6	Probable ATP-dependent RNA helicase DDX6	−1.8	7.59×10^{-2}
P35222	CTNNB1	Catenin beta-1	−2	2.91×10^{-3}
P48637	GSHB	Glutathione synthetase	−2.01	1.74×10^{-1}
Q9NUU7	DD19A	ATP-dependent RNA helicase DDX19A	−2.01	5.06×10^{-2}
P14735	IDE	Insulin-degrading enzyme	−2.01	5.06×10^{-2}
O75533	SF3B1	Splicing factor 3B subunit 1	−2.01	5.06×10^{-2}
Q9P2J5	SYLC	Leucyl-tRNA synthetase	−2.01	5.06×10^{-2}
Q9C0C9	UBE2O	Ubiquitin-conjugating enzyme E2	−2.01	5.06×10^{-2}
P48637	GSHB	Glutathione synthetase	−2.01	5.06×10^{-2}
P61247	RS3A	40S ribosomal protein S3a	−2.16	2.86×10^{-2}
P24752	THIL	Acetyl-CoA acetyltransferase	−2.31	4.97×10^{-2}
P46777	RL5	60S ribosomal protein L5	−2.34	1.73×10^{-1}
A6NC57	ANR62	Ankyrin repeat domain-containing protein 62	−2.34	7.41×10^{-2}
O00764	PDXK	Pyridoxal kinase	−2.34	2.37×10^{-2}
P05386	RLA1	60S acidic ribosomal protein P1	−2.34	2.37×10^{-2}
Q16851	UGPA	UTP–glucose-1-phosphate uridylyltransferase	−2.34	2.37×10^{-2}

Table 1. Continued

Accession	Gene name	Protein name	$\log_2$ ratio	*p*-Value
P78527-2	PRKDC	Isoform 2 of DNA-dependent protein kinase catalytic subunit	−2.34	1.89×10^{-2}
Q14444-2	CAPR1	Isoform 2 of Caprin-1	−2.6	3.34×10^{-2}
P39019	RS19	40S ribosomal protein S19	−2.6	3.34×10^{-2}
P46782	RS5	40S ribosomal protein S5	−2.6	3.34×10^{-2}
P46776	RL27A	60S ribosomal protein L27a	−2.6	3.75×10^{-3}
P62424	RL7A	60S ribosomal protein L7a	−2.6	3.75×10^{-3}
P22626	ROA2	Heterogeneous nuclear ribonucleoproteins A2/B1	−2.69	7.37×10^{-4}
P54886-2	P5CS	Isoform short of delta-1-pyrroline-5-carboxylate synthase	−2.82	5.06×10^{-2}
P09382	LEG1	Galectin-1	−3.02	3.88×10^{-3}
P04181	OAT	Ornithine aminotransferase	−3.92	2.03×10^{-2}
(B) SW480				
P50990	TCPQ	T-Complex protein 1 subunit theta	3.48	3.62×10^{-2}
Q99497	PARK7	Protein DJ-1	2.82	6.62×10^{-3}
P10809	CH60	60 kDa heat shock protein	2.76	1.46×10^{-3}
P04632	CPNS1	Calpain small subunit 1	2.6	3.34×10^{-2}
P49720	PSB3	Proteasome subunit beta type-3	2.6	3.34×10^{-2}
Q15691	MARE1	Microtubule-associated protein RP/EB family member 1	2.34	1.73×10^{-1}
P15559	NQO1	NAD(P)H dehydrogenase [quinone] 1	2.34	7.41×10^{-2}
Q14204	DYHC1	Cytoplasmic dynein 1 heavy chain 1	2.32	6.35×10^{-2}
A8TX70-2	CO6A5	Isoform 2 of collagen alpha-5(VI) chain	2.01	1.74×10^{-1}
Q15648	MED1	Mediator of RNA polymerase II transcription subunit 1	2.01	1.25×10^{-1}
P14314	GLU2B	Glucosidase 2 subunit beta	2.01	5.06×10^{-2}
P49736	MCM2	DNA replication licensing factor MCM2	2.01	5.06×10^{-2}
P49411	EFTU	Elongation factor Tu	1.99	5.06×10^{-2}
P14618	KPYM	Pyruvate kinase isozymes M1/M2	1.82	4.77×10^{-3}
Q13813	SPTA2	Spectrin alpha chain	1.58	1.03×10^{-1}
P22102	PUR2	Trifunctional purine biosynthetic protein adenosine-3	1.58	5.81×10^{-2}
O95373	IPO7	Importin-7	1.58	3.52×10^{-2}
P30041	PRDX6	Peroxiredoxin-6	1.58	9.72×10^{-3}
Q9Y4L1	HYOU1	Hypoxia upregulated protein 1	1.58	8.07×10^{-3}
P19823	ITIH2	Inter-alpha-trypsin inhibitor heavy chain H2	1.58	8.07×10^{-3}
P25788	PSA3	Proteasome subunit alpha type-3	1.58	8.07×10^{-3}
P14174	MIF	Macrophage migration inhibitory factor	1.42	3.75×10^{-3}
Q14152	EIF3A	Eukaryotic translation initiation factor 3 subunit A	1.36	2.66×10^{-3}
Q969J2	ZKSC4	Zinc finger protein with KRAB and SCAN domains 4	1.32	1.74×10^{-1}
P00492	HPRT	Hypoxanthine-guanine phosphoribosyltransferase	1.32	1.25×10^{-1}
P02787	TRFE	Serotransferrin	1.32	5.06×10^{-2}
P52209	6PGD	6-phosphogluconate dehydrogenase, decarboxylating	1.22	1.37×10^{-1}
P53621-2	COPA	Isoform 2 of coatomer subunit alpha	1.01	1.15×10^{-1}
P24534	EF1B	Elongation factor 1-beta	1.01	2.37×10^{-2}
Q01105	SET	Protein SET	−1.01	1.15×10^{-1}
Q9UQ80	PA2G4	Proliferation-associated protein 2G4	−1.01	2.37×10^{-2}
P35222	CTNNB1	Catenin beta-1	−1.06	3.91×10^{-2}
P23396	RS3	40S ribosomal protein S3	−1.09	7.62×10^{-2}
Q7KZF4	SND1	Staphylococcal nuclease domain-containing protein 1	−1.17	6.59×10^{-2}
P05388	RLA0	60S acidic ribosomal protein P0	−1.19	2.67×10^{-2}
P17174	AATC	Aspartate aminotransferase, cytoplasmic	−1.32	1.74×10^{-1}
P17931	LEG3	Galectin-3	−1.32	1.25×10^{-1}
P62988	UBIQ	Ubiquitin	−1.32	5.06×10^{-2}
P62269	RS18	40S ribosomal protein S18	−1.32	6.62×10^{-3}
P55060-3	XPO2	Isoform 3 of exportin-2	−1.39	1.13×10^{-2}
P45974	UBP5	Ubiquitin carboxyl-terminal hydrolase 5	−1.58	8.07×10^{-3}
P46781	RS9	40S ribosomal protein S9	−1.8	1.26×10^{-1}
P15880	RS2	40S ribosomal protein S2	−1.8	4.45×10^{-2}
P62249	RS16	40S ribosomal protein S16	−2.01	1.74×10^{-1}
P12429	ANXA3	Annexin A3	−2.01	5.06×10^{-2}
O14981	BTAF1	TATA-binding protein-associated factor 172	−2.01	5.06×10^{-2}
Q9UNF1	MAGD2	Melanoma-associated antigen D2	−2.01	5.06×10^{-2}
P33992	MCM5	DNA replication licensing factor MCM5	−2.01	5.06×10^{-2}
Q13765	NACA	Nascent polypeptide-associated complex subunit alpha	−2.01	5.06×10^{-2}
P08134	RHOC	Rho-related GTP-binding protein RhoC	−2.01	5.06×10^{-2}
P39023	RL3	60S ribosomal protein L3	−2.01	5.06×10^{-2}
P22626	ROA2	Heterogeneous nuclear ribonucleoproteins A2/B1	−2.01	5.06×10^{-2}
Q9Y5L0	TNPO3	Transportin-3	−2.01	5.06×10^{-2}
Q9BWD1	THIC	Acetyl-CoA acetyltransferase	−2.31	1.16×10^{-2}
P08708	RS17	40S ribosomal protein S17	−2.6	3.34×10^{-2}
P62701	RS4X	40S ribosomal protein S4, X isoform	−2.6	3.34×10^{-2}

Note. The fold change was determined by the ratio of normalized spectral counts of 5-FU: control. Expression ratios are presented as $\log_2$-fold change with associated *p*-values from *t*-test at a significance level of 0.05. For protein groups consisting of proteins with multiple annotated forms identified, only the top scoring form based on MASCOT protein score is represented in the table.

3.6 Antioxidative activity

Oxidative stress is characterized by an imbalance between reactive oxygen species (ROS) generation and the availability of antioxidant species. ROS are thought to be involved in several cellular mechanisms including apoptosis. Studies have shown that many anticancer drugs, including 5-FU, cause cytotoxicity by inducing ROS production [26]. This finding implies that the redox status of the cell is important in determining the sensitivity of cancer cells to chemotherapy.

One of the major mechanisms by which cells protect themselves from this complex situation is through upregulation of a wide range of molecules and enzymes with antioxidant activity. The antioxidant species eliminate ROS to protect the cells from oxidative stress, which may also contribute to chemotherapy drug resistance in cancer. Among these antioxidant species, members of the peroxiredoxin family (Prdxs) of antioxidant enzymes and NAD(P)H:quinone oxidoreductase 1 (NQO1) were shown to be upregulated in the population of colon cancer cells that survived 72 h of 5-FU assault. PRDX2 was more abundant in SW620 while PRDX5 and PRDX6 had higher expression in SW480 5-FU-treated cells as compared to the control cells. Peroxiredoxins (Prdxs) reduce intracellular peroxides such as hydrogen peroxide, one type of ROS, with the thioredoxin system [27]. Prdxs not only play an important role in detoxification, but also increase cell survival and proliferation under conditions of oxidative stress. Furthermore, the detoxification enzyme NQO1 showed increased expression in both SW480 and SW620 cells treated with 5-FU. NQO1 plays a role in chemoprotection by generating antioxidant forms of ubiquinone and vitamin E, which is supported by reports of NQO1 expression in epithelial human tissues, including the colon, that require enhanced levels of antioxidant protection [28]. This cytoprotective enzyme also enhances tumor cell survival during chemotherapy [29]. A Western blot confirmation of the changes in PRDX5 abundance with 5-FU treatment is shown in Fig. 4.

In addition, the SW480 5-FU-treated cells have heightened PARK7 (DJ-1) expression. The oncogene PARK7 is an mRNA-binding protein and sensor for oxidative damage and responds by stabilizing Nrf2. In turn, the transcription factor Nrf2 induces the expression of several antioxidant enzymes including the Prdxs and NQO1 [30]. This may explain the increased levels of these detoxifying enzymes found in the SW480 5-FU surviving cells. There was no change in PARK7 expression between the SW620 5-FU-treated and control cells suggesting that the pathways involved in upregulating antioxidant enzymes may vary as colon cancer progresses. An alternative explanation could be that the original microenvironment for the cell lines has established a differential gene response pattern in the primary versus metastatic cells, as the SW480 and SW620 cell lines are from a primary colon cancer tumor and the lymph node metastasis, respectively. Elevated PARK7 has previously been associated with chemotherapy resistance and poor prognosis in many cancers, but the association of PARK7 with 5-FU resistance and colon cancer is novel.

The colon cancer cells with a higher antioxidant capacity seem to have survived the 5-FU treatment, as these cells were able to survive oxidative damage and apoptosis from 5-FU-induced ROS production. These surviving cells may eventually give rise to a cancer cell population with an acquired resistance to 5-FU through a cellular adaptive response to oxidative stress. The peroxiredoxin family and NQO1 antioxidant enzymes seem to play an important role in 5-FU survival and have the potential to be targets for cancer therapy. Depletion of these enzymes may reduce the cancer cell's ability to scavenge and detoxify ROS, sensitizing the cells to ROS-mediated apoptosis. Although PRDX6 has previously been shown to be upregulated in SW480 cells treated with 5-FU [10], PRDX2, PRDX5, and NQO1 have not been previously associated with 5-FU resistance in colon cancer.

4 Concluding remarks

Using a label-free spectral counting approach to examine response to 5-FU in patient-matched primary and metastatic cell lines, we demonstrated that while some protein patterns are conserved with metastasis, others respond differently. In particular, both the SW480 and SW620 cells experienced changes in their reduction–oxidation response, yet disparate members of the peroxiredoxin family were upregulated following treatment. This result indicates that while the cells experience similar cytotoxic stress, alternative mechanisms are used in response.

Proteomic changes induced by 5-FU treatment in SW480 have previously been examined using 2DE technology followed by MS detection [10]. Although the concentration of 5-FU was double that used in our study, several of the same proteins were found to be increased in expression with treatment. Most notably PRDX6, while nearly threefold increased in expression in our data set, experienced a nearly 11-fold increase with the higher dose of 5-FU [10]. However, there are also several proteins that differ in response between our study and previous literature reports, including two heat shock proteins: heat shock protein beta-1 (P04792) and mitochondrial 60 kDa heat shock protein (P10809). Follow-up studies are needed to examine these discrepancies.

Future studies will include a comparison of label-free approaches with protein-labeling strategies. This study communicates the elucidation of NQO1 antioxidant enzyme and further confirmation of the peroxiredoxin family as possible molecular targets of CRC drug resistance. Further examination into the differential response of primary versus metastatic cells to drug treatment will improve our understanding of the underlying molecular mechanisms and hopefully lead to more effective treatments for this disease.

The authors gratefully acknowledge assistance from the Notre Dame Mass Spectrometry and Proteomics Facility. This research was funded by the University of Notre Dame and the 2011 Starter Grant from the Society for Analytical Chemists of Pittsburgh. K.M.B. was supported by the Notre Dame CBBI program and NIH training grant T32GM075762. P.A.L. was supported by the Notre Dame College of Science REU program.

The authors have declared no conflict of interest.

5 References

[1] AACR Cancer Progress Report: Transforming Patient Care Through Innovation, 2011.

[2] Iwaizumi, M., Tseng-Rogenski, S., Carethers, J. M., DNA mismatch repair proficiency executing 5-fluorouracil cytotoxicity in colorectal cancer cells. *Cancer Biol. Ther.* 2011, *12*, 756–764.

[3] Longley, D. B., Harkin, D. P., Johnston, P. G., 5-fluorouracil: mechanisms of action and clinical strategies. *Nat. Rev. Cancer* 2003, *3*, 330–338.

[4] Bracht, K., Nicholls, A. M., Liu, Y., Bodmer, W. F., 5-fluorouracil response in a large panel of colorectal cancer cell lines is associated with mismatch repair deficiency. *Br. J. Cancer* 2010, *103*, 340–346.

[5] Mechetner, E., Brunner, N., Parker, R. J., In vitro drug responses in primary and metastatic colorectal cancers. *Scand. J. Gastroenterol.* 2011, *46*, 70–78.

[6] Leibovitz, A., Stinson, J. C., McCombs, W. B., 3rd, McCoy, C. E. et al., Classification of human colorectal adenocarcinoma cell lines. *Cancer Res.* 1976, *36*, 4562–4569.

[7] Katayama, M., Nakano, H., Ishiuchi, A., Wu, W. et al., Protein pattern difference in the colon cancer cell lines examined by two-dimensional differential in-gel electrophoresis and mass spectrometry. *Surg. Today* 2006, *36*, 1085–1093.

[8] Xue, H., Lu, B., Zhang, J., Wu, M. et al., Identification of serum biomarkers for colorectal cancer metastasis using a differential secretome approach. *J. Proteome Res.* 2010, *9*, 545–555.

[9] Ghosh, D., Yu, H., Tan, X. F., Lim, T. K. et al., Identification of key players for colorectal cancer metastasis by iTRAQ quantitative proteomics profiling of isogenic SW480 and SW620 cell lines. *J. Proteome Res.* 2011, *10*, 4373–4387.

[10] Wong, C. S., Wong, V. W., Chan, C. M., Ma, B. B. et al., Identification of 5-fluorouracil response proteins in colorectal carcinoma cell line SW480 by two-dimensional electrophoresis and MALDI-TOF mass spectrometry. *Oncol. Rep.* 2008, *20*, 89–98.

[11] Cox, J., Mann, M., Quantitative, high-resolution proteomics for data-driven systems biology. *Annu. Rev. Biochem.* 2011, *80*, 273–299.

[12] Wiese, S., Reidegeld, K. A., Meyer, H. E., Warscheid, B., Protein labeling by iTRAQ: a new tool for quantitative mass spectrometry in proteome research. *Proteomics* 2007, *7*, 340–350.

[13] Everley, P. A., Krijgsveld, J., Zetter, B. R., Gygi, S. P., Quantitative cancer proteomics: stable isotope labeling with amino acids in cell culture (SILAC) as a tool for prostate cancer research. *Mol. Cell. Proteomics* 2004, *3*, 729–735.

[14] Liu, H., Sadygov, R. G., Yates, J. R., 3rd, A model for random sampling and estimation of relative protein abundance in shotgun proteomics. *Anal. Chem.* 2004, *76*, 4193–4201.

[15] Zybailov, B., Coleman, M. K., Florens, L., Washburn, M. P., Correlation of relative abundance ratios derived from peptide ion chromatograms and spectrum counting for quantitative proteomic analysis using stable isotope labeling. *Anal. Chem.* 2005, *77*, 6218–6224.

[16] Neilson, K. A., Ali, N. A., Muralidharan, S., Mirzaei, M. et al., Less label, more free: approaches in label-free quantitative mass spectrometry. *Proteomics* 2011, *11*, 535–553.

[17] Wong, J. W., Cagney, G., An overview of label-free quantitation methods in proteomics by mass spectrometry. *Methods Mol. Biol.* 2010, *604*, 273–283.

[18] Lundgren, D. H., Hwang, S. I., Wu, L., Han, D. K., Role of spectral counting in quantitative proteomics. *Expert Rev. Proteomics* 2010, *7*, 39–53.

[19] Karp, N. A., Spencer, M., Lindsay, H., O'Dell, K. et al., Impact of replicate types on proteomic expression analysis. *J. Proteome Res.* 2005, *4*, 1867–1871.

[20] Nesvizhskii, A. I., Aebersold, R., Interpretation of shotgun proteomic data: the protein inference problem. *Mol. Cell. Proteomics* 2005, *4*, 1419–1440.

[21] Hoehenwarter, W., Wienkoop, S., Spectral counting robust on high mass accuracy mass spectrometers. *Rapid Commun. Mass Spectrom.* 2010, *24*, 3609–3614.

[22] Zhang, Y., Wen, Z., Washburn, M. P., Florens, L., Effect of dynamic exclusion duration on spectral count based quantitative proteomics. *Anal. Chem.* 2009, *81*, 6317–6326.

[23] Old, W. M., Meyer-Arendt, K., Aveline-Wolf, L., Pierce, K. G. et al., Comparison of label-free methods for quantifying human proteins by shotgun proteomics. *Mol. Cell. Proteomics* 2005, *4*, 1487–1502.

[24] Tentes, I. K., Schmidt, W. M., Krupitza, G., Steger, G. G. et al., Long-term persistence of acquired resistance to 5-fluorouracil in the colon cancer cell line SW620. *Exp. Cell Res.* 2010, *316*, 3172–3181.

[25] Singh, A., Settleman, J., EMT, cancer stem cells and drug resistance: an emerging axis of evil in the war on cancer. *Oncogene* 2010, *29*, 4741–4751.

[26] Pelicano, H., Carney, D., Huang, P., ROS stress in cancer cells and therapeutic implications. *Drug Resist. Updates* 2004, *7*, 97–110.

[27] Zhang, B., Wang, Y., Su, Y., Peroxiredoxins, a novel target in cancer radiotherapy. *Cancer Lett.* 2009, *286*, 154–160.

[28] Ross, D., Kepa, J. K., Winski, S. L., Beall, H. D. et al., NAD(P)H:quinone oxidoreductase 1 (NQO1): chemoprotection, bioactivation, gene regulation and genetic polymorphisms. *Chem-Biol. Interact.* 2000, *129*, 77–97.

[29] Siegel, D., Franklin, W. A., Ross, D., Immunohistochemical detection of NAD(P)H:quinone oxidoreductase in human lung and lung tumors. *Clin. Cancer Res.* 1998, *4*, 2065–2070.

[30] Merikallio, H., Paakko, P., Kinnula, V. L., Harju, T. et al., Nuclear factor erythroid-derived 2-like 2 (Nrf2) and DJ1 are prognostic factors in lung cancer. *Hum. Pathol.* 2012, *43*, 577–584.

